NEUROSCIENCE
RESEARCH ARTICLE
J. Kim et al. / Neuroscience 432 (2020) 150–159

Potential Role of the Amygdala and Posterior Claustrum in Exercise Intensity-dependent Cardiovascular Regulation in Rats

Jimmy Kim, [a†] **Ko Yamanaka,** [a†] **Kei Tsukioka** [a,b] **and Hidefumi Waki** [a*]

[a] *Department of Physiology, Graduate School of Health and Sports Science, Juntendo University, Chiba, Japan*

[b] *Japan Society for the Promotion of Science, Tokyo, Japan*

Abstract—Tuning of the cardiovascular response is crucial to maintain performance during high-intensity exercise. It is well known that the nucleus of the solitary tract (NTS) in the brainstem medulla plays a central role in cardiovascular regulation; however, where and how upper brain regions form circuits with NTS and coordinately control cardiovascular responses during high-intensity exercise remain unclear. Here focusing on the amygdala and claustrum, we investigated part of the mechanism for regulation of the cardiovascular system during exercise. In rats, c-Fos immunostaining was used to examine whether the amygdala and claustrum were activated during treadmill exercise. Further, we examined arterial pressure responses to electrical and chemical stimulation of the claustrum region. We also confirmed the anatomical connections between the amygdala, claustrum, and NTS by retrograde tracer injections. Finally, we performed simultaneous electrical stimulation of the claustrum and amygdala to examine their functional connectivity. c-Fos expression was observed in the amygdala and the posterior part of the claustrum (pCL), but not in the anterior part, in an exercise intensity-dependent manner. pCL stimulation induced a depressor response. Using a retrograde tracer, we confirmed direct projections from the amygdala to the pCL and NTS. Simultaneous stimulation of the central nucleus of the amygdala and pCL showed a greater pressor response compared with the stimulation of the amygdala alone. These results suggest the amygdala and pCL are involved in different phases of exercise. More speculatively, these areas might coordinately tune cardiovascular responses that help maintain performance during high-intensity exercise.

Key words: amygdala, claustrum, exercise, nucleus of the solitary tract, cardiovascular regulation, rat.

INTRODUCTION

Proper control of the cardiovascular system is important for exerting and maintaining high-level performance. Parameters such as blood pressure and heart rate are facilitated by exercise intensity, and their activities are autonomically regulated by cardiovascular centers, such as the hypothalamus and brainstem, in the central nervous system (Ludbrook and Graham, 1985; Andresen, 2004; Dampney et al., 2008; Matsukawa, 2012; Waki, 2012; Dampney, 2015).

The nucleus of the solitary tract (NTS) in the medulla oblongata is believed to be a key brain station for cardiovascular control during exercise (Potts, 2006; Michelini and Stern, 2009; Waki, 2012; Michelini et al., 2015). The NTS receives descending central inputs from higher brain areas and ascending inputs from peripheral organs like muscle receptors and baroreceptors (Pilowsky and Goodchild, 2002; Dampney and Horiuchi, 2003; Potts et al., 2003; Benarroch, 2008). In addition, the NTS has projections to the rostral ventrolateral medulla (RVLM), which contains sympathetic premotor neurons, via inhibitory neurons of the caudal ventrolateral medulla (CVLM) (Dampney and Horiuchi, 2003). Supporting these anatomical evidences, glutamatergic excitation of neurons in the NTS has been shown to induce depressor/bradycardic responses (Talman et al., 1980; Leone and Gordon, 1989; Sapru, 2004; Takagishi et al., 2014). Furthermore, treadmill exercise intensity-dependent c-Fos expression has been observed in the rodent NTS (Ohiwa et al., 2006). Thus, NTS may integrate feedforward central commands and feedback peripheral signals to adaptively regulate cardiovascular responses in accordance with exercise intensity. However, the precise

*Corresponding author. Address: Department of Physiology, Graduate School of Health and Sports Science, Juntendo University, 1-1 Hiraka-gakuendai, Inzai, Chiba 270-1695, Japan. Tel: +81-476-98-1001; fax: +81-476-98-1011.
E-mail address: hwaki@juntendo.ac.jp (H. Waki).
† These authors contributed equally to this work.

Abbreviations: aCL, anterior part of the claustrum; BLA, basolateral amygdala; CeA, central nucleus of the amygdala; CL, claustrum; MAP, mean arterial pressure; NTS, nucleus of the solitary tract; pCL, posterior part of the claustrum; RVLM, rostral ventrolateral medulla; CVLM, caudal ventrolateral medulla.

https://doi.org/10.1016/j.neuroscience.2020.02.024
0306-4522/

neuronal mechanism of exercise intensity-dependent cardiovascular regulation remains uncertain.

As a candidate for sending feedforward signals to the NTS and regulating cardiovascular responses during exercise, we focused on the amygdala. We previously reported that electrical and chemical stimulation of the amygdala in anesthetized rats induced bidirectional (facilitatory or inhibitory) cardiovascular responses in a stimulating region-specific manner and an animal physiological state-dependent (chronic/free-moving or acute/anesthesia) manner. Acute microstimulation of the medial region of the central nucleus of the amygdala (CeA; the output station of the amygdala) induced pressor and tachycardiac responses, whereas acute microstimulation of the lateral region of the CeA evoked a depressor response (Yamanaka et al., 2018). Given that the majority of CeA projection neurons contain gamma-aminobutyric acid (i.e. GABAergic neuron) (Pare and Smith, 1993) and have direct projections to the NTS (Rogers and Fryman, 1988), it is possible that the CeA is involved in cardiovascular regulation during exercise.

Furthermore, we focused on the claustrum (CL) as the region that coordinately controls cardiovascular responses along with the amygdala during exercise. The CL is anatomically connected with several cortical (Pearson et al., 1982; Goll et al., 2015; Torgerson et al., 2015; Wang et al., 2017) and subcortical regions including the amygdala (Filimonoff, 1966; Amaral and Insausti, 1992). A recent study investigating input/output connections to and from the CL using transgenic mice reported strong retrograde and anterograde projections between CL and the amygdala, especially its basolateral amygdala (BLA) (Atlan et al., 2018). The functional features for involvement of the CL in arousal (Arnow et al., 2002), attention (Crick and Koch, 2005; Goll et al., 2015), and autonomic cardiovascular regulation via claustro-cortical projections (Hatam et al., 2013; Atlan et al., 2018; Jackson et al., 2018; White et al., 2018) seem important for high-intensity exercise.

Based on these evidences, we hypothesized that the amygdala and CL coordinately control cardiovascular regulation during exercise via NTS projections. To test this hypothesis, we first examined whether the amygdala and CL were activated during exercise using c-Fos immunostaining. Secondly, we investigated arterial pressure responses to electrical and chemical stimulation of CL regions that exhibited exercise intensity-dependent activation. Thirdly, we confirmed anatomical connections between the amygdala, CL, and NTS using a retrograde tracer. Finally, we performed simultaneous electrical stimulation of the CeA and CL to examine functional connectivity.

EXPERIMENTAL PROCEDURES

Animals

Forty-eight male Wistar/ST rats (7–13 weeks old, 276 ± 49 g, Japan SLC, Shizuoka, Japan) were used in this study. Animals were housed in a temperature-controlled room under a fixed 12 h/12 h light/dark cycle (18:00–6:00/6:00–18:00). Food and water were provided *ad libitum*. All experiments were approved by the Ethics Committee for Animal Experiments at Juntendo University and complied with the guidelines of the Physiological Society of Japan.

Telemetric recording of arterial pressure

To investigate cardiovascular parameters during low- and high-intensity exercise, a separate group of rats (n = 6) were anesthetized with isoflurane gas (1.5–2.5%, Pfizer, Japan) using an inhalation anesthesia apparatus (Univentor 400 isoflurane anesthesia unit, Univentor, Zejtun, Malta) and pentobarbital sodium (50 mg/kg) intraperitoneal (i.p.), and implanted with a radio transmitter (HD-S10; Data Sciences International, St. Paul, MN, USA) to record the arterial pressure and body temperature from the abdominal aorta, as reported previously (Waki et al., 2003; Yamanaka et al., 2018). The heart rate was calculated from the arterial pressure data.

Analysis of c-Fos immunolabeling

To examine the specific brain areas involved in neuronal activity dependent on exercise intensity, expression of the proto-oncogene product c-Fos was detected immunohistochemically. Study rats (n = 18) were familiarized with the exercise by treadmill running for 5 days at 10–20 m/min for a period of 30 min one week prior to the experiments. Subsequently, these rats were classified into three groups depending on their running ability: ‘‘high-intensity,’’ ‘‘low-intensity,’’ and ‘‘sedentary.’’ On the day of the experiment, animals in the high-intensity exercise group (n = 6) were placed on the treadmill and made to run at 34 m/min for 60–90 min. Rats in the low-intensity group (n = 6) were placed on the treadmill and made to run 20 m/min for 45 min. Rats in the sedentary group (n = 6) were simply placed on the treadmill with the belt kept stationary. Following this, the animals were returned to their cages and waited for over 60 min from the time reaching the peak of cardiovascular responses occurred during the high-intensity exercise, which was enough time for c-Fos expression in activated regions of the brain (Sharp et al., 1991). Then, the rats were deeply anesthetized by isoflurane, perfused transcardially with heparinized saline followed by 4% paraformaldehyde, and post-fixed in 4% paraformaldehyde. The brain was extracted and sectioned as previously described (Yamanaka et al., 2018). The sections were washed in phosphate-buffered saline (PBS), placed in 10% serum with 0.3% Triton X-100 for 15 min at room temperature, washed once again, and then incubated overnight at 4 °C with anti-c-Fos antibody (sc-52-G; Santa Cruz Biotechnology, Inc., Santa Cruz, CA, USA; 1:200 dilution in PBS with 1% serum and 0.3% Triton X-100). The following day, sections were washed in PBS and incubated with biotinylated horse anti-goat immunoglobulin G (Vector Laboratories, Burlingame, CA, USA; 1:500 dilution) antibody for 1 h. Following another round of washing, the sections were incubated with streptavidin-conjugated Alexa-Fluor 594 (Molecular

Probes, Eugene, OR; 1:500 dilution) for 1 h. Finally, the sections were washed with PBS, mounted on VECTASHIELD (Vector Laboratories), and imaged using a fluorescence microscope (EVOS FL Auto 2 Cell Imaging System, Thermo Fisher Scientific, USA).

The number of c-Fos-positive cells was counted in anterior CL (aCL; 2.3 mm rostral to bregma), posterior CL (pCL), and amygdala sections (1.7 mm caudal to bregma) of each animal. The cell counts were determined by averaging the total cell numbers from each rat per group (high-intensity, low-intensity, and sedentary groups). In each section, the brain regions were delimited according to the rat brain atlas (Paxinos and Watson, 2013). Density was calculated by dividing the cell count by the area. Detection and analysis of c-Fos cells were performed using Image-Pro Premier version 9.3 (Media Cybernetics, Inc. Rockville, MD, USA).

Electrical microstimulation

Arterial pressure and heart rate were monitored and recorded from anesthetized rats as previously described (Takagishi et al., 2014; Yamanaka et al., 2018). Briefly, animals were anesthetized with i.p. urethane (1.45 g/kg). The level of anesthesia was regularly monitored by assessing limb withdrawal response to a noxious pinch; if required, an additional dose of urethane (0.145 g/kg, i.p.) was administered. Rectal temperature was monitored and maintained at 37 °C using a heating pad (BWT-100; Bio Research Center, Nagoya, Japan). The trachea was cannulated to facilitate artificial breathing using a rodent respirator (SN-480-7 Shinano Respirator; Shinano Manufacturing, Tokyo, Japan). A polyethylene catheter (PE-50 tubing filled with heparinized saline) was inserted into the right femoral artery to record the pulsatile arterial pressure. The mean arterial pressure (MAP) and heart rate were derived from the pulsatile pressure signal using a cardiotachometer (AP641-G and AT601-G; Nihon Kohden, Tokyo, Japan). These parameters were simultaneously monitored and recorded using a PowerLab system (PowerLab/8s; ADInstruments, Dunedin, New Zealand). The femoral veins were cannulated with polyethylene tubes (PE-50) for continuous infusion of physiological saline containing the muscle relaxant pancuronium bromide (0.08 mg/kg/h). When the muscle relaxant was used, the adequacy of anesthesia was periodically assessed by observing the arterial pressure response to a noxious stimulus (toe pinch); supplemental urethane (0.145 g/kg i.p.) was administered if required.

Anesthetized rats (n = 6) were placed in a stereotaxic head holder (SR-5; Narishige Scientific Instrument Lab, Tokyo, Japan), and a concentric microelectrode (OA-212-053a; Unique Medical, Tokyo, Japan) was vertically inserted into the right pCL (1.6–2.8 mm caudal, 5.0–6.5 mm lateral to the bregma and 5.0–8.0 mm ventral to the dura). Biphasic negative–positive current pulses (200 μA peak, 0.5 ms pulse, 50 Hz, and 30-s duration) were delivered. After completion of the experiments, the microstimulation sites were marked by electrolytic lesions created by applying a DC current of 1 mA for 5 s. The rats were then intracardially perfused with saline followed by 4% paraformaldehyde. The brains were removed, post-fixed for at least 48 h in 4% paraformaldehyde and sliced into 50 μm serial sections on a freezing microtome (REM-710; Yamato Kohki Industrial, Saitama, Japan). The sections were mounted on slides and imaged using a fluorescence microscope (EVOS FL Auto 2 Cell Imaging System, Thermo Fisher Scientific, USA) to map electrode tracks and lesion marks in the pCL.

Chemical stimulation

A subset of rats (n = 8), different from the ones used for the electrical stimulation experiments were microinjected with the $GABA_A$ antagonist, bicuculline methiodide (1(S),9(R)-(−)-Bicuculline methiodide, 14343, Sigma-Aldrich, St. Louis, MO, USA). The procedures for anesthesia, surgical operations for recording blood pressure and heart rate, and placement on a stereotaxic head holder were same as those of electrical stimulation experiments. Rats were microinjected with bicuculline (n = 4; 0.2–2.0 mM, 0.2 μL) or equivolume saline (n = 4; 0.2 μL, Otsuka Pharmaceutical, Tokushima, Japan) into pCL (1.8 mm caudal, 5.25–5.50 mm lateral to the bregma and 5.0 mm ventral to the dura) using glass micropipettes (outside diameter of 20–30 μm; GC200F-10; Harvard Apparatus, Edenbridge, UK). Micropipettes were connected to a Hamilton microsyringe (1805RN, HAMILTON GASTIGHT Syringes 50 μL, 22S gauge, Reno, NV, USA) on a syringe pump (Legato210P, KD Scientific, Holliston, MA, USA). At the end of the experiment, the injection site was stereotaxically marked by injection of 0.2 μL of fluorescence microspheres (FluoSpheres, Thermo Fisher Scientific, USA).

Anatomical connections among the CeA, pCL and NTS

We used the retrograde tracer fluorogold (hydroxystilbamidine, Biotium, Inc. Hayward, CA, USA) to confirm whether neurons from exercise intensity-dependent brain areas (i.e., CeA and pCL) project directly to the NTS and whether the pCL receives projections from the amygdala. For fluorogold injection, rats were anesthetized with i.p. pentobarbital sodium (50 mg/kg) and isoflurane, placed in a stereotaxic holder, and the dorsal surface of the medulla was exposed. Fluorogold (1 % in H_2O, 50–100 nL injection volume) was unilaterally microinjected into the NTS (n = 3; 0.5–1.0 mm rostral to the calamus scriptorius, 0.4 mm lateral from the midline and at a depth of 0.5 mm from the dorsal surface of the dura on the brainstem) or pCL (n = 3; 1.8 mm caudal and 5.5 mm lateral from the bregma and at a depth of 5.0 mm from the dorsal surface of dura). Animals were then returned to their cages for a recovery period of 7 days. Following this, animals were euthanized, and the brains were extracted and sectioned into 50 μm thick sections. The sections were imaged using a fluorescence microscope as described above section.

Simultaneous stimulation of the CeA and pCL

To understand the functional connections between the CeA and pCL regulating arterial pressure, we performed simultaneous electrical stimulation of the CeA and pCL in four additional rats and then examined the arterial pressure responses. Surgery of anesthetized rats was performed as described above. Two concentric microelectrodes (OA-212-053a; Unique Medical, Tokyo, Japan) were vertically inserted and positioned on the right pCL showing a depressor response (1.8 mm caudal, 5.5 mm lateral to the bregma and 4.0–7.0 mm ventral to the dura) and ipsilateral CeA region showing a pressor response (1.8 mm caudal, 3.0 mm lateral to the bregma, and 6.0–7.0 mm ventral to the dura). Biphasic negative–positive current pulses (200 μA peak, 0.5 ms pulse, 50 Hz, and 30 s duration) were delivered. The effects of stimulation between the single and simultaneous conditions were evaluated on identical locations once the electrode position was fixed.

Statistical analysis

Results are presented as mean ± standard error of the mean (s.e.m.), unless otherwise stated. One-way analysis of variance (ANOVA) with Bonferroni's post-hoc test was used to evaluate the number of cells expressing c-Fos among the high-intensity, low-intensity, and sedentary rat groups. Averaged MAP was traced (mean ± s.e.m., each result calculated from a 2 s bin with a 1 s sliding window) in response to stimulation of the CeA only, pCL only, and both CeA and pCL. Quantification of average maximal ΔMAP (the difference in arterial pressure during stimulation and pre-stimulation) of all stimulation trials was computed from four rats (CeA only: 47 trials, CeA + pCL: 24 trials). To compare cardiovascular responses before and after pCL stimulation and between CeA and pCL stimulation and CeA stimulation only, both Student's paired and unpaired *t*-tests were used after statistical testing for normality distributions (Shapiro–Wilk test) and equal variances (Bartlett's test). If the results did not satisfy these two criteria, non-parametric tests were used (Wilcoxon signed-rank test or Mann–Whitney *U* test). The criterion for statistical significance was set at $p < 0.05$.

RESULTS

Exercise intensity-dependent c-Fos expression occurred in the CeA and posterior CL

We tested whether the amygdala and CL showed neuronal activation during exercise. Animals ($n = 18$) were classified into sedentary (stationary treadmill; $n = 6$), low-intensity (20 m/min; $n = 6$), and high-intensity (34 m/min; $n = 6$) groups. To investigate cardiovascular changes, we recorded the arterial pressure, heart rate, and body temperature during treadmill exercise in a separate group of rats implanted with a telemetric transmitter ($n = 6$). We observed two-phases of change in hemodynamic parameters during high-intensity exercise. In the initial phase of exercise, the arterial pressure and body temperature did not differ between the low- and high-intensity exercise group, although the heart rate increased gradually. However, in the second phase of exercise, the arterial pressure and body temperature during high-intensity exercise dramatically increased 20–30 min before exercise offset (Fig. 1A).

Expression of c-Fos was immunohistochemically visualized in the brain sections of rats subjected to a treadmill running test. Both the amygdala and CL showed robust c-Fos expression during high-intensity exercise (Fig. 1B–D, right panels). The amygdala, including CeA and BLA, and the posterior part of the CL (pCL) showed c-Fos-positive cells in an exercise intensity-dependent manner (Fig. 1B, C, E, F; $p < 0.001$, one-way ANOVA with Bonferroni's post-hoc test), whereas the anterior part of the CL (aCL) showed strong neuronal activation in both exercise groups as well as in the sedentary group (Fig. 1D, G; $p = 0.26$). Interestingly, the amygdala and pCL showed neuronal activation at different exercise levels: the pCL showed significant activation even during low-intensity exercise, whereas the amygdala (particularly CeA) showed significant activation only during high-intensity exercise.

Electrical and chemical stimulation of the pCL induces depressor responses

Previously we showed that electrical microstimulation of the amygdala induced both facilitatory (pressor and tachycardiac) and inhibitory (depressor) cardiovascular responses, specifically at the site of stimulation. Electrical and chemical stimulation of the medial region of the CeA tends to increase arterial pressure and heart rate responses (Yamanaka et al., 2018). In the present study, we examined the effect of pCL microstimulation on cardiovascular responses (Fig. 2A). Unilateral electrical microstimulation (200 μA, 50 Hz and 30 s) of the pCL in urethane-anesthetized rats ($n = 6$) evoked a depressor response. As shown in Fig. 2B, the baseline MAP and heart rate over the 15 s period before stimulation onset were 85.0 ± 1.2 mmHg and 438.6 ± 1.8 bpm, respectively. Stimulation of the pCL induced a decrease in arterial pressure (80.3 ± 2.2 mmHg) but no change in heart rate (434.8 ± 2.0 bpm) (Fig. 2B). Consistent with the results, pCL stimulation evoked decreasing average MAP responses as measured by the change from baseline (ΔMAP) (Fig. 2C left panel, ΔMAP, minimum value ± s.e.m. = −8.3 ± 2.0 mmHg, $t(5) = 4.17$, $p = 0.008$, paired *t*-test) but did not affect the average heart rate from baseline (Δheart rate) (Fig. 2C, right panel, Δheart rate, minimum value ± s.e.m. = −2.2 ± 0.8 bpm, $t(5) = 2.57$, $p > 0.05$, paired *t*-test). Stimulation of areas including the posterior insular cortex surrounding the pCL did not result in significant cardiovascular responses.

In addition, we performed chemical stimulation experiments to test the alternative possibility that depressor responses to pCL electrical microstimulation are caused by stimulating passing fibers, rather than neuronal cell bodies in the pCL (Fig. 2D). Consistent with our electrical stimulation results, microinjection of

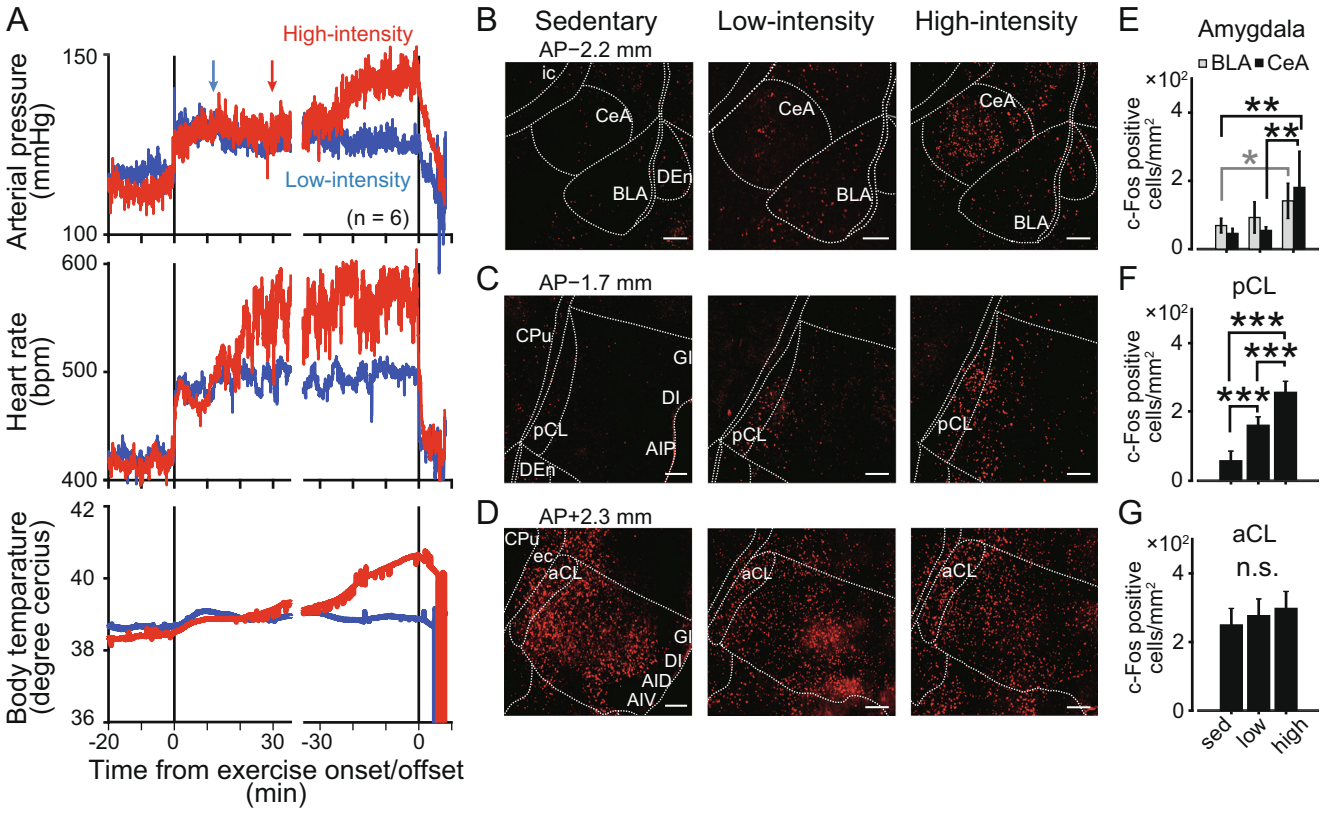

Fig. 1. c-Fos is expressed in an exercise intensity-dependent manner in the amygdala (CeA and BLA) and pCL, but not in the aCL. **(A)** Averaged data of arterial pressure (top panel), heart rate (middle panel), and body temperature (bottom panel) during low- (blue traces) and high-intensity (red traces) treadmill exercise. The blue and red arrows indicate the time point reaching to the setting speed of low- (20 m/min) and high-intensity (34 m/min) exercise, respectively. Physiological parameters were sorted by exercise onset and offset. **(B–G)** Distribution and number (per mm^2) of c-Fos positive cells in sedentary (left panels), low-intensity (middle panels), and high-intensity (right panels) exercise at the level of −2.2 mm **(B, E)**, −1.7 mm **(C, F)**, +2.3 mm **(D, G)** from the bregma. Scale bar = 200 μm. *$p < 0.05$, **$p < 0.01$, ***$p < 0.001$. AID, agranular insular cortex, dorsal part; AIP, agranular insular cortex, posterior part; AIV, agranular insular cortex, ventral part; BLA, basolateral amygdala; CeA, central nucleus of the amygdala; aCL, anterior part of the claustrum; CPu, caudate putamen (striatum); DEn, dorsal endopiriform nucleus; DI, dysgranular insular cortex; ec, external capsule; GI, granular insular cortex; GP, globus pallidus; ic, internal capsule; pCL, posterior part of the claustrum.

bicuculline (0.2–2 mM, 0.2 μL), a $GABA_A$ antagonist, into the pCL induced prolonged depressor responses (Fig. 2E and F left panel, ΔMAP, mean value ± s.e.m. = −13.0 ± 2.3 mmHg, $t(3) = 2.56$, $p = 0.04$, unpaired *t*-test) compared to saline injection (ΔMAP, mean value ± s.e.m. = −2.0 ± 3.6 mmHg), but not significant heart rate changes (Fig. 2F, right panel, bicuculline: Δheart rate, mean value ± s.e.m. = −17.6 ± 17.1 bpm; saline: Δheart rate, mean value ± s.e.m. = 13.7 ± 9.9 bpm, $t(3) = 1.58$, $p > 0.05$, unpaired *t*-test).

Therefore, in contrast to the results after CeA stimulation with pressor response, stimulation of the pCL induced depressor response.

Anatomical connections among the CeA, pCL and NTS

Next, we examined whether the pCL region with depressive effects had anatomical connections with the NTS and amygdala. The retrograde tracer fluorogold, which was unilaterally microinjected (50–100 nL) into the NTS of rats ($n = 3$), was detected after a period of seven days in the ipsilateral medial division of the CeA (CeM), but not the pCL (Fig. 3A–C). A recent study using genetic tools reported that the CL has reciprocal connections to the amygdala (Atlan et al., 2018). To confirm the anatomical connections between the amygdala and pCL region, which induced inhibitory cardiovascular responses, we also injected fluorogold into the pCL depressor region (1.8 mm caudal, 5.5 mm lateral from the bregma and 5.0 mm ventral from the dura) in three rats. Fluorescence was observed in the BLA but not the CeA (Fig. 3D, E). Consistent with previous work (Atlan et al., 2018), these results support that the CeA (especially CeM) neurons project directly to the NTS, but not the pCL, whereas, BLA neurons project directly to the pCL depressor region.

Simultaneous electrical stimulation of CeA and pCL

Stimulation of the pCL or CeA (particularly medial region) using a single electrode evoked depressor (this study) or pressor/tachycardiac (Yamanaka et al., 2018) cardiovascular responses, respectively. As shown in Fig. 1, neuronal activation of the amygdala (BLA and CeA) and pCL displayed different exercise levels, indicating that only pCL neurons were activated during low-intensity exercise, whereas both amygdala and pCL neurons were

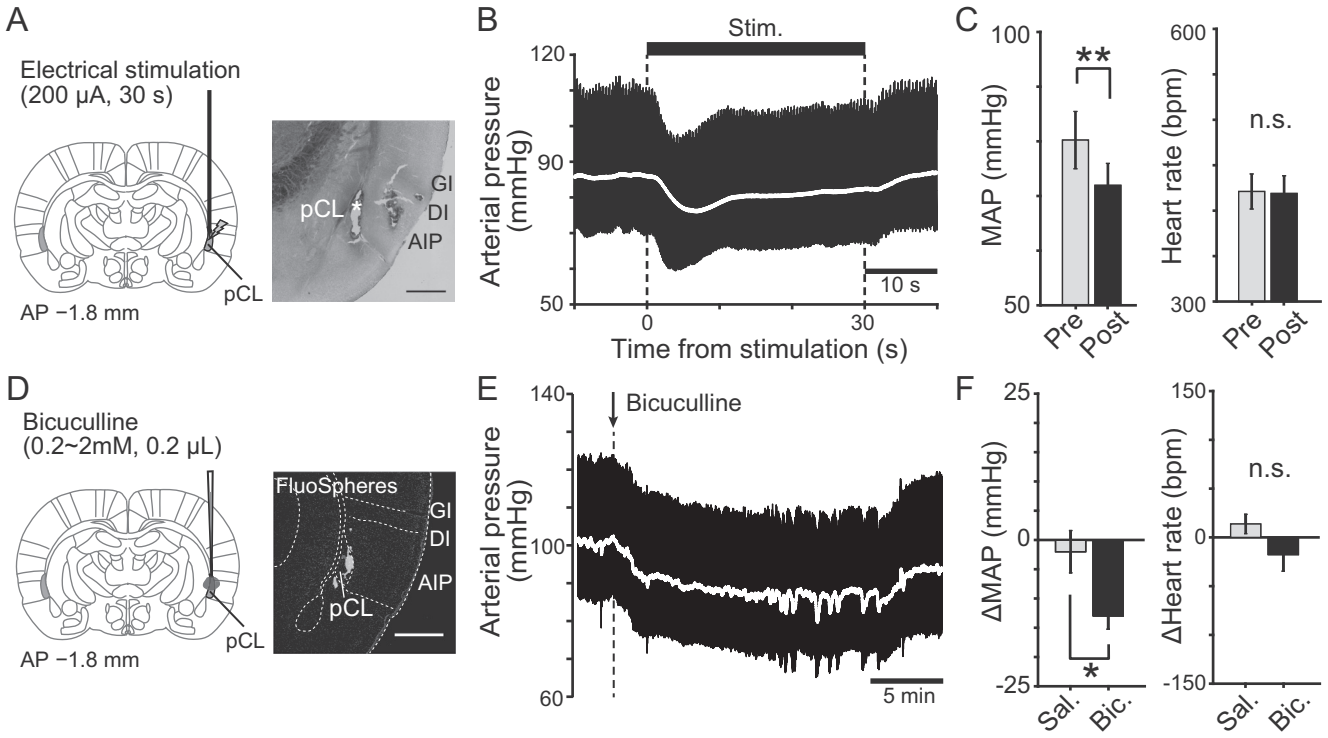

Fig. 2. Electrical and chemical stimulation of the posterior claustrum induced a depressor response. **(A)** A concentric microelectrode was unilaterally penetrated for electrical microstimulation of pCL in anesthetized rats (left panel). Histological image of the electrolytic lesion mark (*) in pCL by passing a positive DC current of 1 mA for 5 s, and microelectrode track in neighboring areas including insular cortex for verifying location of the stimulation site (right panel). **(B)** A representative trace of the arterial pressure before and after pCL microstimulation (200 μA, 50 Hz, 30 s). **(C)** Averaged data show pCL microstimulation induced inhibitory responses on the arterial pressure but not on the heart rate. **(D)** Glass capillary loaded $GABA_A$ antagonist bicuculline 0.2 μL was inserted into the right pCL (left panel). Histological image of the injection site using fluorescent microspheres (FluoSpheres, 0.2 μL) (right panel). **(E, F)** Same as **(B)** and **(C)** respectively, but before and after microinjection of bicuculline into the pCL. *$p < 0.05$, **$p < 0.01$, paired *t*-test **(C)** and unpaired *t*-test **(F)** were used. Scale bar on photograph of histology **(A, D)**, 1 mm. AIP, agranular insular cortex, posterior part; DI, dysgranular insular cortex; GI, granular insular cortex; pCL, posterior part of the claustrum.

activated during high-intensity exercise. To mimic the state of amygdala and pCL neuronal activities during high-intensity exercise, we performed simultaneous electrical microstimulation of the CeA and pCL regions using two microelectrodes (Fig. 4A) in four rats. Consistent with previous results, single stimulation of the CeA and pCL consistently induced pressor (Fig. 4B red line) and depressor (Fig. 4B cyan line) responses. Surprisingly, despite the position of the two electrodes was not changed between stimulation conditions, simultaneous microstimulation of the CeA and pCL resulted in significantly greater pressor responses (Fig. 4B black line; ΔMAP, median maximum value ± s.e.m. = 10.8 ± 0.8 mmHg, $U(47,24) = 321$, $Z = 2.95$, $p = 0.003$, Mann–Whitney *U* test) compared with CeA stimulation alone (ΔMAP, median maximum value ± s.e.m. = 6.2 ± 0.6 mmHg).

DISCUSSION

The amygdala (CeA and BLA) and pCL showed exercise intensity-dependent c-Fos expression. pCL neurons were activated both during low- and high-intensity exercise, whereas amygdala neurons were activated only during high-intensity exercise. Additionally, microstimulation of the pCL or CeA in anesthetized rats induced contrasting responses, i.e. depressor and no-heart rate change or pressor and tachycardiac cardiovascular responses, respectively. Thus, CeA and pCL outputs adjust activation of the sympathetic, rather than parasympathetic, nervous system. Since the level of sympathetic nervous system activity is known to increase during exercise (Miki et al., 2002; Matsukawa, 2012) and is correlated with fatigue (Saito et al., 1989), it is a possible that amygdala and pCL neurons distinctly yet coordinately contribute to the maintenance of exercise performance by sympathoexcitation (e.g., energy supply to active skeletal muscles) and suppression of sympathetic nervous system activity.

Given the c-Fos expression results during high-intensity exercise and the anatomical connections between the pCL and amygdala, we simultaneously stimulated the CeA and pCL, which resulted in a greater pressor response compared with stimulation of the CeA alone. This result is counterintuitive because CeA or pCL stimulation induced pressor or depressor responses, respectively, as linearly which should be counterbalanced during a simultaneous stimulation. It is assumed that the amygdala and pCL have direct or indirect projections to a cardiovascular output station like the NTS and RVLM (Schwaber et al., 1982; van der Kooy et al., 1984; Rogers and Fryman, 1988; Danielsen et al., 1989; Wallace et al., 1989; Liubashina et al., 2000), whereas the BLA has reciprocal connections to the pCL (Filimonoff, 1966; Amaral and Insausti, 1992;

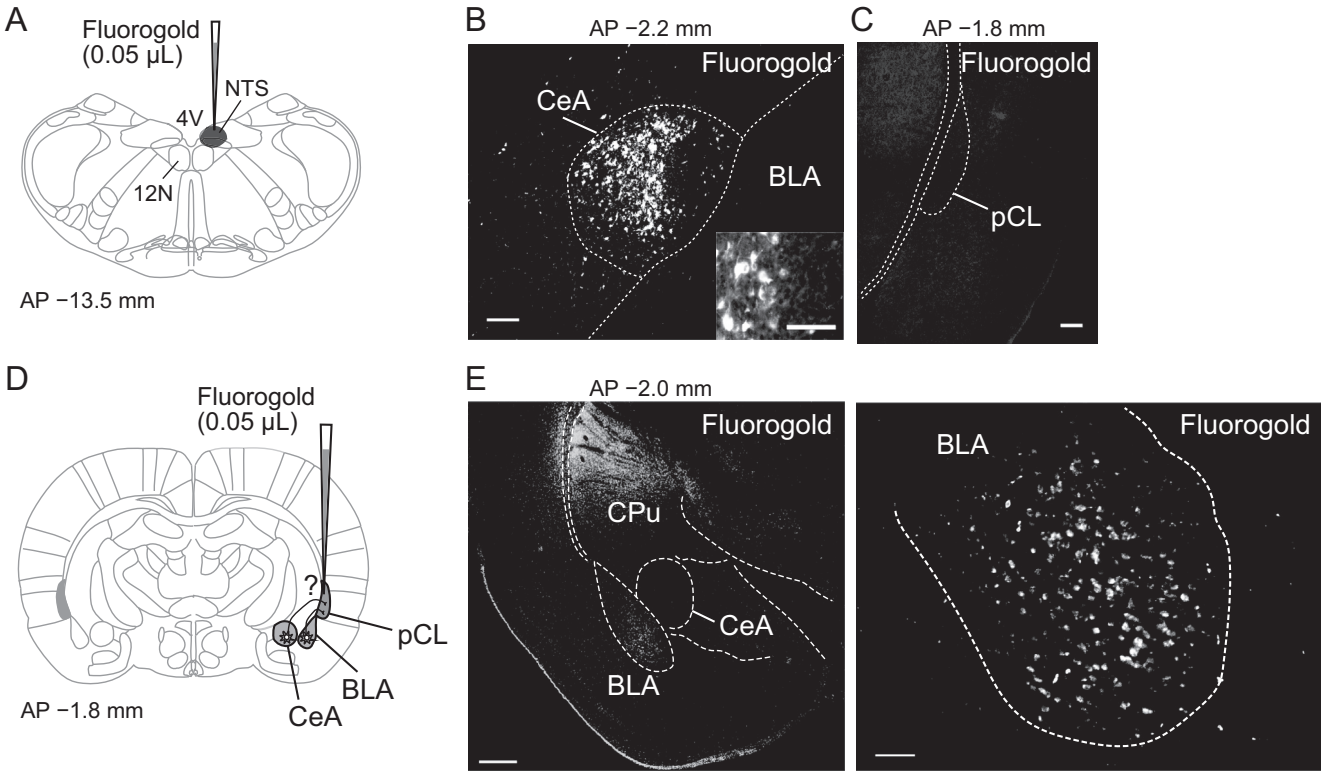

Fig. 3. Anatomical connections among the CeA, pCL and NTS were confirmed using a retrograde tracer. **(A)** Fluorogold, a retrograde tracer, was microinjected into the NTS. **(B)** Fluorogold was observed in the CeA, particularly in the medial region (CeM). Inset: A magnified image of fluorogold-positive CeA neurons. Histological image at 2.2 mm caudal from the bregma. **(C)** Same as **(B)**. However, fluorescence was not detected in pCL. Brain slice at 1.8 mm caudal from the bregma. **(D)** Fluorogold was microinjected into the pCL to confirm anatomical inputs from the amygdala. **(E)** Fluorogold expression was detected in the BLA, but not in the CeA (left panel). A magnified image of the BLA (right panel). Scale bar = 0.2 mm in (B, C, and E right panel), 0.1 mm in (B) inset, and 1 mm in (E, left panel). BLA, basolateral amygdala; CeA, central nucleus of the amygdala; CPu, caudate putamen; pCL, posterior part of the claustrum.

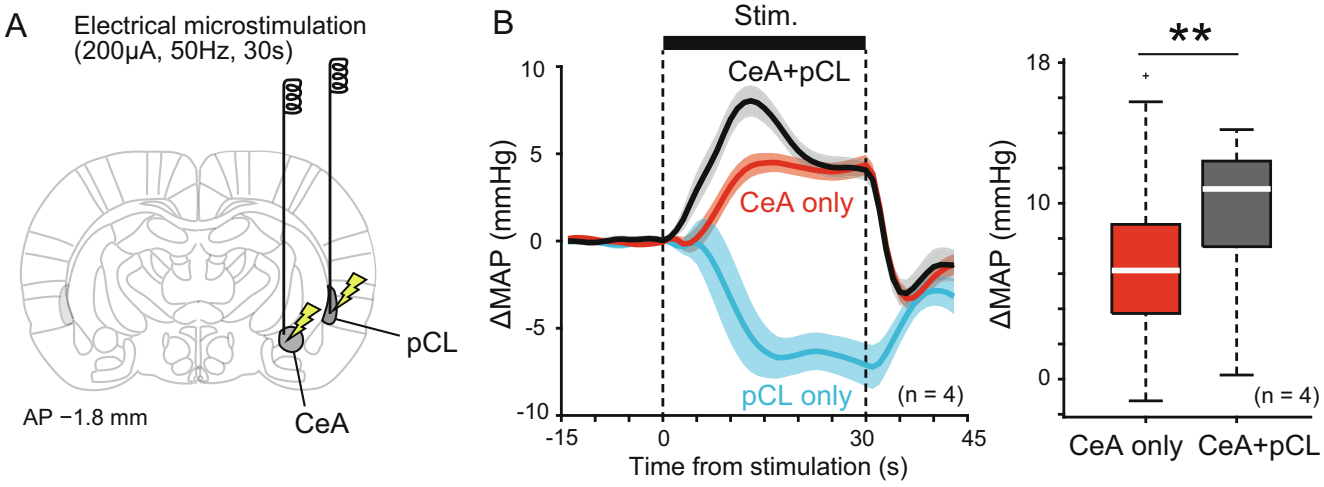

Fig. 4. Simultaneous stimulation of the CeA and pCL mimics activities during exercise induced non-linearly pressor responses. **(A)** Two stimulation electrodes were inserted into CeA (−1.8 mm caudal, 3.0 mm lateral from bregma, 6.5–7.5 mm ventral from dura) and pCL (1.8–2.2 mm caudal, 5.5–6.0 mm lateral from bregma, 5.0–7.0 mm ventral from dura). The intensity and duration of electrical stimulation and electrode position were identical between single and simultaneous stimulation. **(B)** Left panel: Averaged ΔMAP (difference of arterial pressure during stimulation and pre-stimulation) traces (mean ± s.e.m., each datapoint was calculated by a 2 s bin with a 1 s sliding window) in response to stimulation of the CeA only (red line), pCL only (cyan line), and both CeA + pCL (black line). Right panel: Box plot for quantification of average ΔMAP of all stimulation trials (CeA only: 47 trials, CeA + pCL: 24 trials, from 4 rats). Red and gray bars indicate trials of CeA only stimulation and CeA + pCL stimulation, respectively. $^{**}p < 0.01$, Mann-Whitney *U* test.

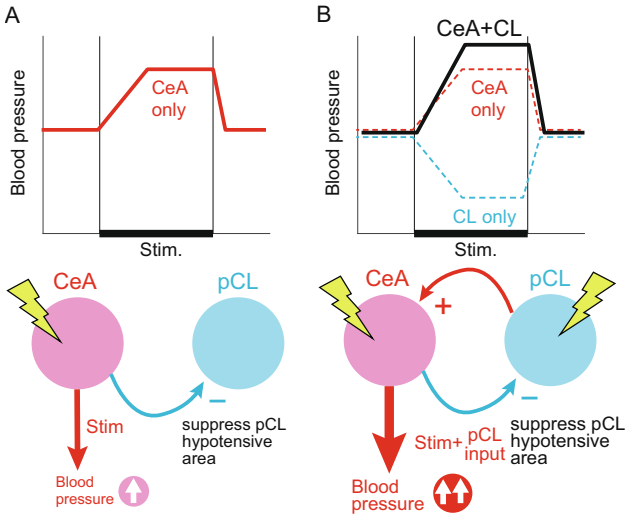

Fig. 5. Hypothetical schema of the functional interaction between the amygdala and claustrum. The simultaneous electrical stimulation of CeA and pCL (**(B)**, "CeA + CL"; ex. high-intensity exercise *in vivo*) induced stronger pressor responses than stimulation of CeA alone (**(A)**, "only CeA"). Excitatory inputs from pCL to CeA may also induce additional increases in blood pressure, and inhibitory inputs from CeA to pCL may suppress the hypotensive area of the pCL.

Atlan et al., 2018). A state of low-intensity exercise accompanied by a low stress level activates the pCL, but not the amygdala. On the other hand, under conditions of high stress such as during high-intensity exercise, both the amygdala and pCL are activated. Our anatomical and physiological evidence suggests that a functional interaction between the amygdala and claustrum has the role of excitatory projections from the pCL to the CeA (promoting the activity of the CeA pressor area), and conversely, inhibitory projections from the CeA to the pCL (suppressing of the activity of the pCL hypotensive area), via BLA (Fig. 5).

What are the mechanisms for activating these circuits during high-intensity exercise? It is reasonable to consider that the involvement of ascending and descending systems: feedforward signals from central command as a descending system (Goodwin et al., 1972), and feedback inputs from peripheral receptors. The current understanding of the central command processes is that they originate from motor-related cortical and subcortical areas; such as the prefrontal cortex, hypothalamus and mesencephalic locomotor regions (Jansen et al., 1995; Koba et al., 2018; Liang et al., 2016; Williamson et al., 2003). The amygdala may be incorporated into these central command circuits; it is well known to be involved in defense reactions and to have descending pathways into the brainstem locomotor regions and cardiorespiratory regions (Hilton and Zbrozyna, 1963; van der Kooy et al., 1984; Rogers and Fryman, 1988; Wallace et al., 1989). While for ascending mechanisms from peripheral inputs, previous study suggested that CeA receives nociceptive signals that could be involved in the emotional-affective and autonomic reactions to pain processes (Bernard et al., 1992). Furthermore, the amygdala may detect pH attenuation (acidosis) and rising CO_2 concentrations (Ziemann et al., 2009). During high-intensity exercise, these chemical and metabolic reactions coupled to stress may define exercise limitations as a result of over-activation of the amygdala, excessive sympathetic nerve activity, and restricted blood flow to active muscles.

Overall, in this study, we observed consistent and strong activation of the aCL in an exercise intensity-independent manner. A previous study reported that chemical stimulation of the aCL elicited a depressor response and that the effect was significantly reduced by inactivation of the medial prefrontal cortex (Hatam et al., 2013). There are differences between the anatomical connections of the claustro-cortical and claustro-subcortical projections along the rostro-caudal axis (Goll et al., 2015). Recent studies have reported the importance of claustro-cortical projections in cognitive functions (Barbas et al., 2003; Smith and Alloway, 2010; Brown et al., 2017; Jackson et al., 2018; White et al., 2018). Although the role of the claustro-subcortical projection is obscure, it may serve as a hub linking autonomic regulation and processing arousing events, such as flight behavior during an emergency, in cooperation with the subcortical system, e.g., noradrenaline neurons of the locus coeruleus (Aston-Jones and Cohen, 2005; Burgess and Peever, 2013) or histamine neurons of the hypothalamic tuberomammillary nucleus (Bhuiyan et al., 2011; Takagishi et al., 2014; Yamanaka et al., 2017).

This study is subject to several limitations. First, we used electrical microstimulation to mimic CeA and pCL activity during exercise *in vivo*. A benefit of electrical microstimulation is the high temporal resolution for switching of a single or simultaneous stimulation of subcortical structures, whereas a downside is that electrical microstimulation may stimulate the cell body as well as passing fibers at the stimulation sites. A second limitation is that we used forced treadmill exercise; thus, it is difficult to separate the effects of exercise, stress, or both. In our protocol, we found that exercise intensity, especially in high-intensity exercise, induces c-Fos expression not only in claustrum and amygdala but also other brain regions such as in hypothalamus, midbrain and brainstem (data not shown). The functions of these regions are unclear and require future studies. Finally, in this study, we observed cardiovascular responses induced by stimulation of CeA and pCL in anesthetized rats. We have not directly tested the relationship between the blood pressure or heart rate responses and the number of c-Fos expressing neurons in the amygdala and claustrum during exercise. Therefore, we could not approach the causality whether the exercise intensity-dependent co-activations of the amygdala and pCL contribute cardiovascular control during exercise. Future studies could examine the relationship between amygdala and pCL activities as well as cardiovascular variables, and whether c-Fos-expressing neurons project to the NTS by parallel usage of c-Fos immunohistochemistry and tracing methods. More directly, it is necessary that the pCL-CeA-NTS pathway-specific manipulations in awake exercising animals by targeted lesions of pCL, CeA, and NTS, by functional disconnection techniques using

asymmetrical lesions (Hart et al., 2018), and by genetic methods such as optogenetics and chemogenetics.

In conclusion, we demonstrated that the CL, particularly the pCL, and the amygdala coactivated and may be coordinately involved in cardiovascular tuning during high-intensity treadmill exercise. Amygdala and pCL showed strong c-Fos expression during high-intensity exercise. Stimulation of the pCL region alone evoked depressor effects. We also confirmed the anatomical connections between the amygdala, pCL, and NTS. Simultaneous microstimulation of both the CeA and pCL induced enhanced pressor effects compared with stimulation of the CeA alone. We speculate that functional linkage of the CeA and pCL might be involved in coordinated tuning of cardiovascular regulation in an exercise intensity-dependent manner. Taken together, our data provide novel insights into the central mechanisms underlying autonomic cardiovascular regulation during, especially high-intensity, exercise.

AUTHOR CONTRIBUTIONS

J.K., K.Y. and H.W. designed this research; J.K., K.Y., K. T. and H.W. performed experiment; J.K. and K.Y. analyzed the data; and J.K., K.Y, and H.W. wrote the paper.

ACKNOWLEDGEMENTS

The study was financially supported by the Japan Society for the Promotion of Science KAKENHI grants 16K16485 (to K.Y.), the joint research program of Juntendo University, Faculty of Health and Sports Science (to J. K.), MEXT-Supported Program for the Strategic Research Foundation at Private Universities, 2014–2018 (S1411008; to H.W.), and Private University Research Branding Project (to H.W.). We thank M. Takagishi and Y. Hasegawa for technical support.

CONFLICT OF INTEREST

The authors declare no conflict of interest.

REFERENCES

Amaral DG, Insausti R (1992) Retrograde transport of D-[3H]-aspartate injected into the monkey amygdaloid complex. Exp Brain Res 88:375–388.

Andresen MC (2004) Cardiovascular integration in the nucleus of the solitary tract. In: Dun NJ, Machado BH, Pilowsky PM, editors. Neural mechanisms of cardiovascular regulation. Boston: Kluwer Academic Publishers. p. 59–80.

Arnow BA, Desmond JE, Banner LL, Glover GH, Solomon A, Polan ML, Lue TF, Atlas SW (2002) Brain activation and sexual arousal in healthy, heterosexual males. Brain 125:1014–1023.

Aston-Jones G, Cohen JD (2005) An integrative theory of locus coeruleus-norepinephrine function: adaptive gain and optimal performance. Annu Rev Neurosci 28:403–450.

Atlan G, Terem A, Peretz-Rivlin N, Sehrawat K, Gonzales BJ, Pozner G, Tasaka GI, Goll Y, et al. (2018) The claustrum supports resilience to distraction. Curr Biol.

Barbas H, Saha S, Rempel-Clower N, Ghashghaei T (2003) Serial pathways from primate prefrontal cortex to autonomic areas may influence emotional expression. BMC Neurosci 4:25.

Benarroch EE (2008) The arterial baroreflex: functional organization and involvement in neurologic disease. Neurology 71:1733–1738.

Bernard JF, Huang GF, Besson JM (1992) Nucleus centralis of the amygdala and the globus pallidus ventralis: electrophysiological evidence for an involvement in pain processes. J Neurophysiol 68:551–569.

Bhuiyan ME, Waki H, Gouraud SS, Takagishi M, Kohsaka A, Maeda M (2011) Histamine receptor H1 in the nucleus tractus solitarii regulates arterial pressure and heart rate in rats. Am J Physiol Heart Circ Physiol 301:H523–529.

Brown SP, Mathur BN, Olsen SR, Luppi PH, Bickford ME, Citri A (2017) New breakthroughs in understanding the role of functional interactions between the neocortex and the claustrum. J Neurosci 37:10877–10881.

Burgess CR, Peever JH (2013) A noradrenergic mechanism functions to couple motor behavior with arousal state. Curr Biol.

Crick FC, Koch C (2005) What is the function of the claustrum? Philos Trans R Soc Lond B Biol Sci 360:1271–1279.

Dampney RA (2015) Central mechanisms regulating coordinated cardiovascular and respiratory function during stress and arousal. Am J Physiol Regul Integr Comp Physiol 309:R429–443.

Dampney RA, Horiuchi J (2003) Functional organisation of central cardiovascular pathways: studies using c-fos gene expression. Prog Neurobiol 71:359–384.

Dampney RA, Horiuchi J, McDowall LM (2008) Hypothalamic mechanisms coordinating cardiorespiratory function during exercise and defensive behaviour. Auton Neurosci 142:3–10.

Danielsen EH, Magnuson DJ, Gray TS (1989) The central amygdaloid nucleus innervation of the dorsal vagal complex in rat: a Phaseolus vulgaris leucoagglutinin lectin anterograde tracing study. Brain Res Bull 22:705–715.

Filimonoff IN (1966) The claustrum, its origin and development. J Hirnforsch 8:503–528.

Goll Y, Atlan G, Citri A (2015) Attention: the claustrum. Trends Neurosci.

Goodwin GM, McCloskey DI, Mitchell JH (1972) Cardiovascular and respiratory responses to changes in central command during isometric exercise at constant muscle tension. J Physiol 226:173–190.

Hart G, Bradfield LA, Balleine BW (2018) Prefrontal corticostriatal disconnection blocks the acquisition of goal-directed action. J Neurosci 38:1311–1322.

Hatam M, Sheybanifar M, Nasimi A (2013) Cardiovascular responses of the anterior claustrum; its mechanism; contribution of medial prefrontal cortex. Auton Neurosci 179:68–74.

Hilton SM, Zbrozyna AW (1963) Amygdaloid region for defence reactions and its efferent pathway to the brain stem. J Physiol 165:160–173.

Jackson J, Karnani MM, Zemelman BV, Burdakov D, Lee AK (2018) Inhibitory control of prefrontal cortex by the claustrum. Neuron 99. 1029–1039 e1024.

Jansen AS, Nguyen XV, Karpitskiy V, Mettenleiter TC, Loewy AD (1995) Central command neurons of the sympathetic nervous system: basis of the fight-or-flight response. Science 270:644–646.

Koba S, Hanai E, Kumada N, Kataoka N, Nakamura K, Watanabe T (2018) Sympathoexcitation by hypothalamic paraventricular nucleus neurons projecting to the rostral ventrolateral medulla. J Physiol.

Leone C, Gordon FJ (1989) Is L-glutamate a neurotransmitter of baroreceptor information in the nucleus of the tractus solitarius? J Pharmacol Exp Ther 250:953–962.

Liang N, Mitchell JH, Smith SA, Mizuno M (2016) Exaggerated sympathetic and cardiovascular responses to stimulation of the mesencephalic locomotor region in spontaneously hypertensive rats. Am J Physiol Heart Circ Physiol 310:H123–131.

Liubashina O, Jolkkonen E, Pitkanen A (2000) Projections from the central nucleus of the amygdala to the gastric related area of the dorsal vagal complex: a Phaseolus vulgaris-leucoagglutinin study in rat. Neurosci Lett 291:85–88.

Ludbrook J, Graham WF (1985) Circulatory responses to onset of exercise: role of arterial and cardiac baroreflexes. Am J Physiol 248:H457–467.
Matsukawa K (2012) Central command: control of cardiac sympathetic and vagal efferent nerve activity and the arterial baroreflex during spontaneous motor behaviour in animals. Exp Physiol 97:20–28.
Michelini LC, Stern JE (2009) Exercise-induced neuronal plasticity in central autonomic networks: role in cardiovascular control. Exp Physiol 94:947–960.
Michelini LC, O'Leary DS, Raven PB, Nobrega AC (2015) Neural control of circulation and exercise: a translational approach disclosing interactions between central command, arterial baroreflex, and muscle metaboreflex. Am J Physiol Heart Circ Physiol 309:H381–392.
Miki K, Kosho A, Hayashida Y (2002) Method for continuous measurements of renal sympathetic nerve activity and cardiovascular function during exercise in rats. Exp Physiol 87:33–39.
Ohiwa N, Saito T, Chang H, Nakamura T, Soya H (2006) Differential responsiveness of c-Fos expression in the rat medulla oblongata to different treadmill running speeds. Neurosci Res 54:124–132.
Pare D, Smith Y (1993) Distribution of GABA immunoreactivity in the amygdaloid complex of the cat. Neuroscience 57:1061–1076.
Paxinos G, Watson C (2013) The rat brain in stereotaxic coordinates. 7th ed. Academic Press.
Pearson RC, Brodal P, Gatter KC, Powell TP (1982) The organization of the connections between the cortex and the claustrum in the monkey. Brain Res 234:435–441.
Pilowsky PM, Goodchild AK (2002) Baroreceptor reflex pathways and neurotransmitters: 10 years on. J Hypertens 20:1675–1688.
Potts JT (2006) Inhibitory neurotransmission in the nucleus tractus solitarii: implications for baroreflex resetting during exercise. Exp Physiol 91:59–72.
Potts JT, Paton JF, Mitchell JH, Garry MG, Kline G, Anguelov PT, Lee SM (2003) Contraction-sensitive skeletal muscle afferents inhibit arterial baroreceptor signalling in the nucleus of the solitary tract: role of intrinsic GABA interneurons. Neuroscience 119:201–214.
Rogers RC, Fryman DL (1988) Direct connections between the central nucleus of the amygdala and the nucleus of the solitary tract: an electrophysiological study in the rat. J Auton Nerv Syst 22:83–87.
Saito M, Mano T (1989) Iwase S., Sympathetic nerve activity related to local fatigue sensation during static contraction. J Appl Physiol (1985) 67:980–984.
Sapru HN (2004) Neurotransmitters in the nucleus tractus solitaries mediating cardiovascular function. In: Dun NJ, Machado BH, Pilowsky PM, editors. Neural mechanisms of cardiovascular regulation. Boston: Kluwer Academic Publishers. p. 81–98.
Schwaber JS, Kapp BS, Higgins GA, Rapp PR (1982) Amygdaloid and basal forebrain direct connections with the nucleus of the solitary tract and the dorsal motor nucleus. J Neurosci 2:1424–1438.
Sharp FR, Sagar SM, Hicks K, Lowenstein D, Hisanaga K (1991) c-fos mRNA, Fos, and Fos-related antigen induction by hypertonic saline and stress. J Neurosci 11:2321–2331.
Smith JB, Alloway KD (2010) Functional specificity of claustrum connections in the rat: interhemispheric communication between specific parts of motor cortex. J Neurosci 30:16832–16844.
Takagishi M, Gouraud SS, Bhuiyan ME, Kohsaka A, Maeda M, Waki H (2014) Activation of histamine H1 receptors in the nucleus tractus solitarii attenuates cardiac baroreceptor reflex function in rats. Acta Physiol (Oxf) 211:73–81.
Talman WT, Perrone MH, Reis DJ (1980) Evidence for L-glutamate as the neurotransmitter of baroreceptor afferent nerve fibers. Science 209:813–815.
Torgerson CM, Irimia A, Goh SY, Van Horn JD (2015) The DTI connectivity of the human claustrum. Hum Brain Mapp 36:827–838.
van der Kooy D, Koda LY, McGinty JF, Gerfen CR, Bloom FE (1984) The organization of projections from the cortex, amygdala, and hypothalamus to the nucleus of the solitary tract in rat. J Comp Neurol 224:1–24.
Waki H (2012) Central mechanisms of cardiovascular regulation during exercise: Integrative functions of the nucleus of the solitary tract. J Phys Fitness Sports Med 1:253–261.
Waki H, Kasparov S, Wong LF, Murphy D, Shimizu T, Paton JF (2003) Chronic inhibition of endothelial nitric oxide synthase activity in nucleus tractus solitarii enhances baroreceptor reflex in conscious rats. J Physiol 546:233–242.
Wallace DM, Magnuson DJ, Gray TS (1989) The amygdalo-brainstem pathway: selective innervation of dopaminergic, noradrenergic and adrenergic cells in the rat. Neurosci Lett 97:252–258.
Wang Q, Ng L, Harris JA, Feng D, Li Y, Royall JJ, Oh SW, Bernard A, et al. (2017) Organization of the connections between claustrum and cortex in the mouse. J Comp Neurol 525:1317–1346.
White MG, Panicker M, Mu C, Carter AM, Roberts BM, Dharmasri PA, Mathur BN (2018) Anterior cingulate cortex input to the claustrum is required for top-down action control. Cell reports 22:84–95.
Williamson JW, McColl R, Mathews D (2003) Evidence for central command activation of the human insular cortex during exercise. J Appl Physiol (1985) 94:1726–1734.
Yamanaka K, Gouraud SS, Takagishi M, Kohsaka A, Maeda M, Waki H (2017) Evidence for a histaminergic input from the ventral tuberomammillary nucleus to the solitary tract nucleus involved in arterial pressure regulation. Physiol Rep 5 e13095.
Yamanaka K, Takagishi M, Kim J, Gouraud SS, Waki H (2018) Bidirectional cardiovascular responses evoked by microstimulation of the amygdala in rats. J Physiol Sci 68:233–242.
Ziemann AE, Allen JE, Dahdaleh NS, Drebot II, Coryell MW, Wunsch AM, Lynch CM, Faraci FM, et al. (2009) The amygdala is a chemosensor that detects carbon dioxide and acidosis to elicit fear behavior. Cell 139:1012–1021.

(Received 6 October 2019, Accepted 17 February 2020)
(Available online 26 February 2020)